A STREAMWISE-CONSTANT MODEL OF TURBULENT PIPE FLOW

Jean-Loup Bourguignon
Graduate Aerospace Laboratories
California Institute of Technology
1200 E. California Blvd, Pasadena, California 91125, U.S.A.
jeanloup@caltech.edu

Beverley J. McKeon
Graduate Aerospace Laboratories
California Institute of Technology
1200 E. California Blvd, Pasadena, California 91125, U.S.A.
mckeon@caltech.edu

ABSTRACT

We present a streamwise-constant model of turbulent pipe flow forced by stochastic noise and focus particularly on the influence of the no-slip boundary condition in the azimuthal direction on the flow behavior. With a no-slip boundary condition at the wall, our model captures the formation of "streamwise-constant puffs", so-called due to the good agreement between the temporal evolution of their velocity field and the projection of the velocity field associated with three-dimensional puffs in a frame of reference moving at the bulk velocity. The three-dimensional puffs were observed experimentally by Hof *et al.* (2004) and Nishi *et al.* (2008), and simulated numerically by Shimizu & Kida (2009). When we allow for slip in the azimuthal direction, we no longer observe the quasi-periodic generation of puffs, instead the flow stays away from the laminar state for extended periods of time. We observe that, for a given forcing amplitude, a larger blunting of the velocity profile is realized when we allow for slip in the azimuthal direction and we relate this larger amplification to the existence of self-sustained solutions of the linearized streamfunction equation with slip at the wall.

INTRODUCTION

Streamwise-elongated structures have been shown to play an important role in pipe flow transition (van Doorne & Westerweel, 2009), as well as in fully developed turbulence (Kim & Adrian, 1999; Morrison *et al.*, 2004; Guala *et al.*, 2006), and take the form of quasi-streamwise vortices and streaks of the axial velocity. Pipe flow transition is a two-step process (Mellibovsky *et al.*, 2009) characterized by the generation of puffs followed by their expansion in space and merging, leading to fully developed turbulence. The puffs correspond to the flow response to large amplitude disturbances at low Reynolds number and are characterized by a sharp trailing edge and a smooth leading edge (Wygnanski & Champagne, 1973). The dominant flow structures inside a puff are quasi-streamwise vortices and streaks, as observed in the particle-image-velocimetry (PIV) measurements of Hof *et al.* (2004), and are independent of the method used to generate the puff (Wygnanski & Champagne, 1973). The velocity profile inside a puff exhibits a blunter shape compared to laminar which is typical of pipe flow turbulence.

Linear models of pipe flow, e.g. Schmid & Henningson (1994), capture the general characteristics of the large-scale structures that play an important role in the flow dynamics but are unable to reproduce the change in mean flow associated with the transition to turbulence. The presence of nonlinear terms is required in order to obtain a blunting of the velocity profile. The 2D/3C model for Couette flow by Gayme *et al.* (2010), so called because it describes the evolution of the three components of velocity in a plane perpendicular to the mean flow direction, successfully captures the blunting of the velocity profile and turbulence intensities.

A 2D/3C model for the pipe was derived from the Navier-Stokes (NS) equations by Joseph & Tao (1963) and is significantly simpler and more tractable than the 3-dimensional Navier-Stokes equations. Inspired by the work of Gayme *et al.* (2010) we add small-amplitude stochastic forcing to the 2D/3C model, which takes into account the perturbations present in experiments as well as unmodelled effects. The background noise is highly amplified by the flow due to the non-normality of the governing operator (Reddy & Ioannou, 2000), resulting in the generation of streamwise vortices which convect axial momentum to create streaks. An innovative feature of our model, as explained in Bourguignon & McKeon (2011), is the convection of the streaks in the radial direction by the action of the nonlinearities, which leads to a change in mean flow reflecting the transition to turbulence.

In the following sections, we present the streamwise-constant model for pipe flow and the numerical methods used to simulate the flow. We describe the response of our model to stochastic forcing, considering at first no-slip boundary conditions (BCs) and then allowing for slip in the azimuthal di-

rection. We relate our results to the difference in amplification obtained using deterministic forcing of the streamwise momentum equation with either a slip or a no-slip BC in the azimuthal direction. We then study the time evolution of a streamwise-constant puff before summarizing the main achievements described in this paper.

PRESENTATION OF THE MODEL

The 2D/3C model consists of two evolution equations, one for the streamfunction Ψ describing the in-plane velocities and one for the axial velocity u_x deviating from laminar, i.e. $u_x = \tilde{u}_x - U$, where $\tilde{u}_x$ is the instantaneous axial velocity and U is the laminar base flow. We only force the streamfunction equation, based on the study of Jovanovic & Bamieh (2005) which showed that maximum amplification is obtained by forcing in the cross-sectional plane. The 2D/3C model is written

$$\begin{cases} \frac{\partial \Delta\Psi}{\partial \tau} = \frac{2}{Re}\Delta^2\Psi + \mathscr{N}_\psi \\ \frac{\partial u_x}{\partial \tau} = C - \frac{1}{\eta}\frac{\partial \Psi}{\partial \phi}\frac{\partial U}{\partial \eta} - \frac{1}{\eta}\frac{\partial \Psi}{\partial \phi}\frac{\partial u_x}{\partial \eta} + \frac{1}{\eta}\frac{\partial \Psi}{\partial \eta}\frac{\partial u_x}{\partial \phi} + \frac{2}{Re}\Delta u_x \\ \Psi|_{\eta=1} = \frac{\partial \Psi}{\partial \eta}|_{\eta=1} = 0 \end{cases} \tag{1}$$

where $\Delta = \frac{1}{\eta}\left(\frac{\partial}{\partial \eta}\left(\eta \frac{\partial}{\partial \eta}\right) + \frac{1}{\eta}\frac{\partial^2}{\partial \phi^2}\right)$ is the 2D Laplacian. The boundary conditions are no-slip and no-penetration on the wall of the pipe. The bulk velocity is maintained constant by adjusting the pressure gradient C. The streamfunction equation is linearized in order to obtain the simplest model able to capture the blunting of the velocity profile and also because the study of Gayme *et al.* (2010) showed no significant differences in the Couette flow statistics obtained using either a nonlinear or a linearized streamfunction equation.

NUMERICAL METHODS

The governing equations for the streamwise vorticity and velocity are solved numerically on a 2D domain using a pseudo-spectral collocation method. The spectral expansion is based on Fourier modes in the azimuthal direction and Chebyshev polynomials in the radial direction. The singularity at the origin of the polar coordinate system is avoided by redefining the radius from -1 to 1 and using an even number of grid points in the radial direction, as in Heinrichs (2004). The two partial differential equations are solved in physical space, i.e. the unknowns are the streamwise vorticity and velocity at each grid point, with homogeneous boundary conditions $\omega_x = 0$ and $u_x = 0$ at the wall. The streamfunction is obtained by solving the discretized Laplace equation $\Delta\Psi = -\omega_x$ associated with homogeneous boundary conditions corresponding to no-penetration at the wall. The no-slip BC in the azimuthal direction is enforced by adding particular solutions to the streamfunction with non-zero vorticity at the wall, following the influence matrix method for linear equations, see Peyret (2002), such that the azimuthal velocity $u_\phi = -\frac{\partial \Psi}{\partial \eta}$ vanishes at the wall.

We solve the discretized partial differential equations in time, starting from the laminar state, using a third-order semi-implicit time stepping scheme described in Spalart *et al.* (1991). The code is written in Fortran and relies on an optimized solver for Sylvester type equations from the SLICOT numerical library (Jonsson & Kagstrom, 2003). The bulk velocity is maintained constant by adjusting the pressure gradient during the simulation. We use $N = 48$ grid points in the radial direction and $M = 96$ grid points in the azimuthal direction for the low forcing amplitude and or low Re simulations and $N = 64$, $M = 128$ grid points otherwise. The time step is set to 10^{-3} dimensionless time units. The flow properties considered in this study were shown to be independent of the choice of temporal and spatial discretizations by running comparative tests at higher spatial resolution and using smaller time steps.

The governing equation for the streamfunction is subject to the stochastic forcing term $\mathscr{N}_\psi$ which is approximated numerically by adding white noise at each grid point in space and at every time step. The stochastic forcing follows a normal distribution with zero mean and a variance that depends on the radius such that the variance per surface area is constant. The square root of the variance, i.e. the forcing root mean square (rms) amplitude, is set to 5×10^{-4} and 2×10^{-3} respectively for the small and large forcing amplitude simulations. In order to prevent aliasing to appear when we compute the nonlinear coupling terms in the streamwise velocity equation, we truncate the 2D Fourier transform of the forcing term after the lowest two-third wavenumbers, see Canuto (2006).

The in-plane kinetic energy $v^2 + w^2$, axial kinetic energy u^2, and centerline velocity are saved at each time step and the full flow field is saved every 4 dimensionless time units. The centerline velocity is approximated by averaging the axial velocity in the azimuthal direction over the grid points closest to the center of the pipe. The simulation parameters and boundary conditions are summarized in Table 1.

Table 1. Simulation parameters, boundary conditions (BCs), mean in-plane turbulent kinetic energy $\frac{1}{t_s}\int_0^{t_s} v^2 + w^2 dt$ ($A_{N,\Psi}$) and amplification factor from the in-plane velocities to the streamwise velocity ($A_{\Psi,u}$) defined as $\frac{1}{t_s}\int_0^{t_s} \frac{u^2}{v^2+w^2} dt$, where t_s is the simulation duration of 2000 dimensionless time units.

Re	Forcing (rms)	BCs	$A_{N,\Psi}$	$A_{\Psi,u}$
2,200	5×10^{-4}	no-slip	2.8×10^{-4}	120
2,200	2×10^{-3}	no-slip	9.1×10^{-3}	17
10,000	5×10^{-4}	no-slip	1.1×10^{-3}	336
10,000	2×10^{-3}	no-slip	3.8×10^{-3}	137
10,000	5×10^{-4}	slip	2.4×10^{-4}	1932
10,000	2×10^{-3}	slip	2.3×10^{-3}	201

RESULTS

Streamwise-Constant Puff Signatures and Amplification Factor

The time traces of the centerline velocity scaled by the bulk velocity for the simulations with no-slip and no-penetration BCs at $Re = 2,200$ and $Re = 10,000$ are shown respectively on Figure 1(a),(b) and Figure 2(a),(b). The time traces exhibit sharp drops followed by a smooth recovery nearly back to the laminar value. We identify the sharp drops as the signature of "streamwise-constant puffs" and define a puff timescale as the time elapsed between two sharp drops. The average puff timescale increases linearly with the Reynolds number and corresponds to 75 dimensionless time units based on the pipe radius and bulk velocity at $Re = 2,200$ and 330 at $Re = 10,000$. A puff timescale of 75 dimensionless time units compares well with experimental data, e.g. in Nishi *et al.* (2008), the puffs are 5 to 20 diameters long depending on Reynolds number and convect at nearly the bulk velocity. A puff of length $20D$ which is separated from the next puff by a laminar region of length equivalent to one puff would lead to a dimensionless timescale based on the pipe radius of 80. Increasing the forcing amplitude results in more pronounced puff signatures as can be seen on Figure 2(b) compared to Figure 2(a). The time average in-plane kinetic energy defined as $\frac{1}{t_s}\int_0^{t_s} v^2 + w^2 dt$, where t_s is the simulation duration of 2000 dimensionless time units, and the time average amplification factor between the in-plane kinetic energy and the streamwise kinetic energy given by $\frac{1}{t_s}\int_0^{t_s} \frac{u^2}{v^2+w^2} dt$ are reported on Table 1. The amplification factor increases with the Reynolds number for a given forcing amplitude and decreases with increasing forcing amplitude at constant Reynolds number due to nonlinear saturation. Note that we do not observe any scaling trend of the in-plane kinetic energy with the Reynolds number for a given forcing amplitude. The instantaneous amplification factor, given by the ratio of the streamwise kinetic energy to the in-plane kinetic energy is plotted as a function of time on Figure 1(c),(d) and Figure 2(c),(d) and exhibits oscillations at the same frequency as the puff signatures in the centerline velocity. The maxima of the amplification factor are approximately in phase with the sharp drops of the centerline velocity.

When we allow for slip in the azimuthal direction, keeping the no-slip BC in the streamwise direction and no-penetration at the wall of the pipe, we observe that the time traces of the centerline velocity do not exhibit clear puff signatures as is the case for no-slip BCs. The centerline velocity stays away from the laminar value during extended periods of time, as can be seen on Figure 3(a),(b). We observe that under stochastic forcing with slip in the azimuthal direction, the streamwise-constant simulations do not periodically come back to the laminar state but instead stay away from the laminar state sometimes during more than 1000 dimensionless time units at $Re = 10,000$. The mean value of the centerline velocity scaled by the bulk velocity for a forcing amplitude of 2×10^{-3} is 1.45 compared to 1.70 for the simulation with no-slip BCs at the same Reynolds number and forcing amplitude and 1.26 for fully developed turbulence at the same Reynolds number (den Toonder & Nieuwstadt, 1997). At low forcing amplitude the amplification factor is 6 times larger than with no-slip BCs but at larger forcing amplitude the amplification factors are of the same order of magnitude. We can justify this increase in amplification factor at low forcing amplitude by the fact that due to the slip condition at the wall the streamwise vortices can reach closer to the wall and convect near-wall low-momentum fluid further from the wall therefore enhancing the streamwise-momentum redistribution resulting in the blunting of the velocity profile. At larger forcing amplitude, we can argue that the vortices are strong enough to efficiently redistribute streamwise-momentum regardless of the boundary condition and that nonlinear saturation prevents the continued increase of the amplification factor, therefore limiting the gain obtained by allowing for slip in the azimuthal direction.

In order to further investigate the difference in the flow behavior when we change the azimuthal boundary condition from no-slip to slip, we consider forcing the streamwise momentum equation by a given streamfunction $\Psi(\eta,\phi) = \Psi_1(\eta)\sin\phi$, where $\Psi_1(\eta)$ is expressed as a Taylor series at the origin, i.e. $\Psi_1 = \sum_{i=0}^{\infty} \alpha_i \eta^i$. We set $\alpha_0 = 0$ in order to enforce continuity in the limit of η tending to zero, recalling that $\Psi(\eta,\phi) = -\Psi(\eta,\phi+\pi)$, and $\alpha_2 = 0$ in order for the forcing profile to be bounded at the origin. The forcing profile generating Ψ_1 is given by

$$N(\eta) = -\frac{1}{Re}\left(\partial_{\eta\eta} + \frac{1}{\eta}\partial_\eta - \frac{1}{\eta^2}\right)^2 \Psi_1(\eta) \qquad (2)$$

The lowest order streamfunction satisfying the no-penetration boundary condition at the wall is $\Psi(\eta,\phi) = \alpha(\eta - \eta^3)\sin\phi$ with slip at the wall in the azimuthal direction and $\Psi(\eta,\phi) = \alpha(\eta - 3\eta^3 + 2\eta^4)\sin\phi$ with no-slip. The associated forcing profiles $N(\eta)$ are respectively $N(\eta) = 0$ and $N(\eta) = -\frac{90\alpha}{Re}$. The streamfunction with slip at the wall is an exact solution of the unforced linearized streamfunction equation. In order to satisfy the no-slip condition, we need to keep higher order terms in the Taylor series expansion of the streamfunction and these terms result in a non-zero forcing. The existence of self-sustained solutions with slip at the boundary might justify why we get larger amplification in our stochastically forced simulations since infinitely small forcing can triger a self-sustained solution and result in order one change in mean flow whereas infinitely small forcing with a no-slip BC in the azimuthal direction will only lead to a change in mean flow proportional to the disturbance amplitude.

Time Evolution of a Streamwise-Constant Puff

We consider the time evolution of the flow during one cycle corresponding to the generation of a streamwise-constant puff followed by its slow decay and the return of the flow close to the laminar state. The three main stages in the evolution of a streamwise-constant puff are plotted on Figure 4**(a)** to **(f)** and the time instants when the snapshots were taken are indicated on Figure 1. The evolution of a streamwise-constant puff is described in details in Bourguignon & McKeon (2011) and is remarkably similar to the flow visualizations by Hof *et al.* (2004) in transitioning pipe flow when a puff is observed in a reference frame moving at the bulk velocity. The cycle starts with the formation of streamwise vortices inside the domain, due to the stochastic forcing, and at the wall, in order to satisfy the no-slip boundary condition. The vortices move away

from the wall **4(d), (e)** and create streaks by advection of the mean shear **4(a)**. The low-speed streaks, defined with respect to the laminar base flow, convect towards the center whereas the high-speed streaks stay near the wall, resulting in a blunting of the velocity profile characteristic of turbulent pipe flow **4(b)**. Maximum blunting is obtained when a low-speed streak reaches the center of the pipe, resulting in a sharp drop of the centerline velocity, and is followed by the slow decay of the streamwise vortices and streaks **4(c),(f)** and the return of the flow close to the laminar state.

CONCLUSIONS

We presented a streamwise-constant model for turbulent pipe flow and focused on the influence of the no-slip boundary condition on the flow dynamics. Under stochastic forcing and with no-slip and no-penetration boundary conditions at the wall of the pipe the time traces of the centerline velocity exhibit sharp drops followed by a smooth recovery nearly back to the laminar value. The sharp drops of the centerline velocity occur quasi-periodically and are associated with the signature of streamwise-constant puffs. When we allow for slip in the azimuthal direction the clear puff signatures are no longer present and the flow stays away from the laminar state during extended periods of time instead of coming back close to the laminar state quasi-periodically as is the case with the no-slip condition. A deterministic model for both the slip and no-slip cases was introduced and the unforced streamfunction equation in the model exhibits an analytic solution with slip at the wall. We argued that the large amplification observed with slip boundary condition is related to the existence of self-sustained solutions.

The support of AFOSR grant # FA 9550-09-1-0701 (program manager John Schmisseur) is gratefully acknowledged.

REFERENCES

Bourguignon, J-L. & McKeon, B. J. 2011 A streamwise-constant model of turbulent pipe flow. *Submitted* .

Canuto, C. 2006 *Spectral methods: fundamentals in single domains*. Springer-Verlag.

van Doorne, C. W. H. & Westerweel, J. 2009 The flow structure of a puff. *Phil. Trans. Royal Soc. A* **367**, 489–507.

Gayme, D., McKeon, B. J., Papachristodoulou, A., Bamieh, B. & Doyle, J. C. 2010 A streamwise constant model of turbulence in plane Couette flow. *J. Fluid Mech.* **658**, 99–119.

Guala, M., Hommema, S. E. & Adrian, R. J. 2006 Large-scale and very-large-scale motions in turbulent pipe flow. *J. Fluid Mech.* **554**, 521–542.

Heinrichs, W. 2004 Spectral collocation schemes on the unit disc. *J. Comp. Phys.* **199** (1), 66–86.

Hof, B., van Doorne, C. W. H., Westerweel, J., Nieuwstadt, F. T. M., Faisst, H., Eckhardt, B., Wedin, H., Kerswell, R. R. & Waleffe, F. 2004 Experimental observation of nonlinear traveling waves in turbulent pipe flow. *Science* **305** (5690), 1594–1598.

Jonsson, I. & Kagstrom, B. 2003 RECSY - A high performance library for Sylvester-type matrix equations. *Euro-Par 2003 Parallel Processing, Proceedings* **2790**, 810–819.

Joseph, D. D. & Tao, L. N. 1963 Transverse velocity components in fully developed unsteady flows. *J. Appl. Mech.* pp. 147–148.

Jovanovic, M. R. & Bamieh, B. 2005 Componentwise energy amplification in channel flows. *J. Fluid Mech.* **534**, 145–183.

Kim, K. C. & Adrian, R. J. 1999 Very large-scale motion in the outer layer. *Phys. Fluids* **11** (2), 417–422.

Mellibovsky, F., Meseguer, A., Schneider, T. M. & Eckhardt, B. 2009 Transition in localized pipe flow turbulence. *Phys. Rev. Letters* **103**.

Morrison, J. F., Jiang, W., McKeon, B. J. & Smits, A. J. 2004 Scaling of the streamwise velocity component in turbulent pipe flow. *J. Fluid Mech.* **508**, 99–131.

Nishi, M., Uensal, B., Durst, F. & Biswas, G. 2008 Laminar-to-turbulent transition of pipe flows through puffs and slugs. *J. Fluid Mech.* **614**, 425–446.

Peyret, R. 2002 *Spectral methods for incompressible viscous flow*, *Applied mathematical sciences*, vol. 148. Springer.

Reddy, S. C. & Ioannou, P. J. 2000 Energy transfer analysis of turbulent plane Couette flow. *Proceedings of the IUTAM Laminar-Turbulent Transition* pp. 211–216.

Schmid, P. J. & Henningson, D. S. 1994 Optimal energy density growth in Hagen-Poiseuille flow. *J. Fluid Mech.* **277**, 197–225.

Shimizu, M. & Kida, S. 2009 A driving mechanism of a turbulent puff in pipe flow. *Fluid Dynam. Res.* **41**.

Spalart, P. R., Moser, R. D. & Rogers, M. M. 1991 Spectral methods for the Navier-Stokes equations with one infinite and two periodic directions. *J. Comp. Phys.* **96** (2), 297–324.

den Toonder, J. M. J. & Nieuwstadt, F. T. M. 1997 Reynolds number effects in a turbulent pipe flow for low to moderate Re. *Phys. Fluids* **9** (11), 3398–3409.

Wygnanski, I. J. & Champagne, F. H. 1973 On transition in a pipe. Part 1: The origin of puffs and slugs and the flow in a turbulent slug. *J. Fluid Mech.* **59**, 281–335.

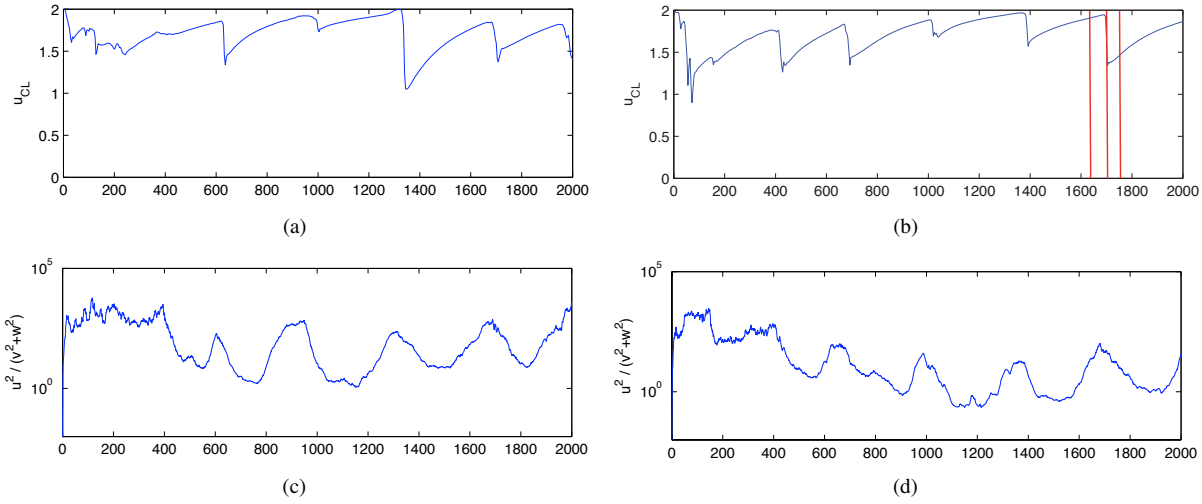

Figure 1. Time traces of the centerline velocity (a), (b) and amplification factor $u^2/(v^2+w^2)$ (c), (d) from two different simulations at $Re = 10,000$ with respectively 0.0005 and 0.002 rms noise levels. The vertical lines (b) indicate the time instants when the samples of Figure 4 are taken.

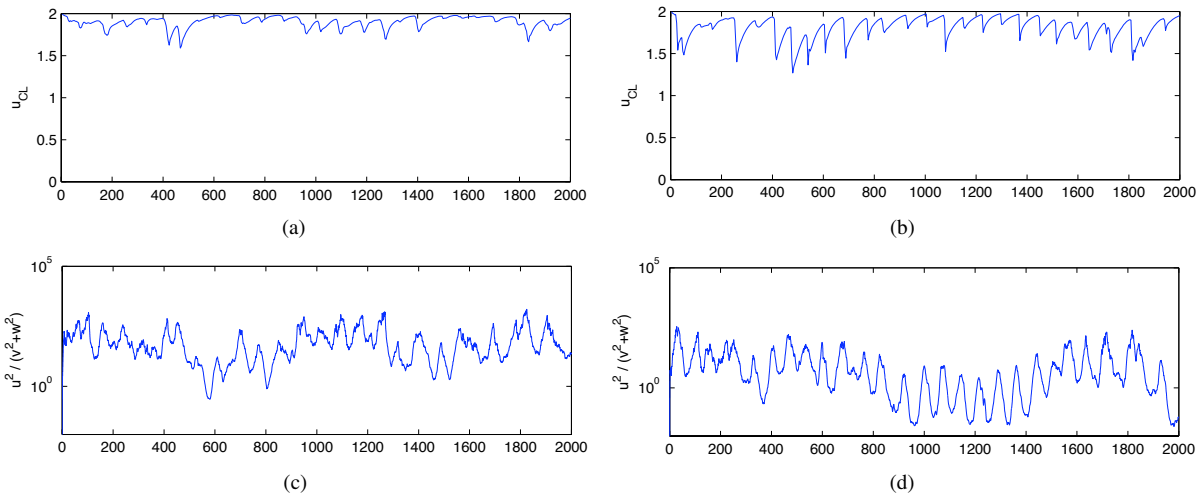

Figure 2. Time traces of the centerline velocity (a), (b) and amplification factor $u^2/(v^2+w^2)$ (c), (d) from two different simulations at $Re = 2,200$ with respectively 0.0005 and 0.002 rms noise levels

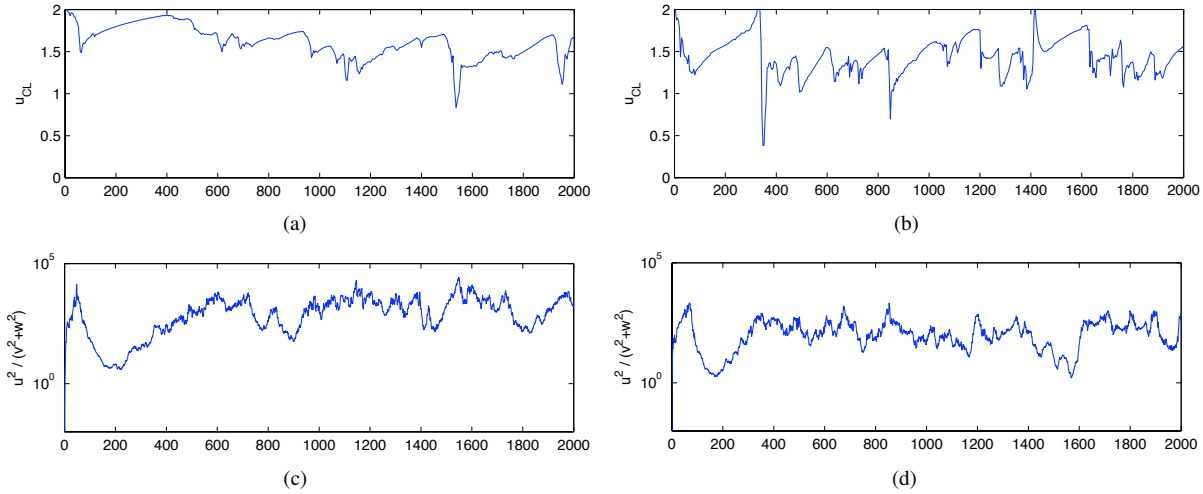

Figure 3. Time traces of the centerline velocity (a), (b) and amplification factor $u^2/(v^2+w^2)$ (c), (d) from two different simulations at $Re = 10,000$ with respectively 0.0005 and 0.002 rms noise levels and with slip boundary condition at the wall of the pipe.

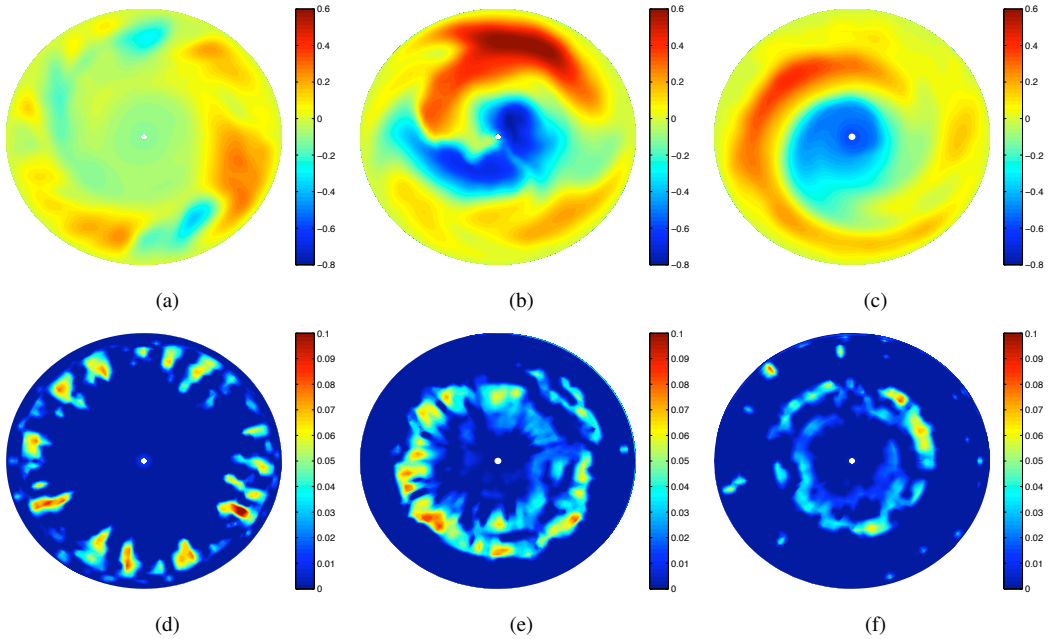

Figure 4. Contours of the axial velocity, subfigures (a) to (c), and of the swirling strength for the in-plane velocities, subfigures (d) to (f), computed respectively at $t = 1620$, $t = 1700$, and $t = 1740$. The swirling strength is defined as the magnitude of the imaginary part of the in-plane velocity gradient eigenvalues.